Influence of uniaxial anisotropy on domain wall motion driven by spin torque

P. Chureemart,[1,*] R. F. L. Evans,[2] I. D'Amico,[2] and R. W. Chantrell[2]

[1]*Computational and Experimental Magnetism Group, Department of Physics, Mahasarakham University, Mahasarakham 44150, Thailand*

[2]*Department of Physics, University of York, York YO10 5DD, United Kingdom*

(Received 19 April 2015; revised manuscript received 15 July 2015; published 25 August 2015)

Magnetization dynamics of a bilayer structure in the presence of a spin-transfer torque is studied using an atomistic model coupled with a model of spin accumulation. The spin-transfer torque is decomposed into two components: adiabatic and nonadiabatic torques, expressed in terms of the spin accumulation, which is introduced into the atomistic model as an additional field. The evolution of the magnetization and the spin accumulation are calculated self-consistently. We introduce a spin-polarized current into a material containing a domain wall whose width is varied by changing the anisotropy constant. It is found that the adiabatic spin torque tends to develop in the direction of the magnetization whereas the nonadiabatic spin torque arising from the mistracking of conduction electrons and local magnetization results in out-of-plane magnetization components. However, the adiabatic spin torque significantly dominates the dynamics of the magnetization. The total spin-transfer torque acting on the magnetization increases with the anisotropy constant due to the increasing magnetization gradient.

DOI: 10.1103/PhysRevB.92.054434 PACS number(s): 75.78.Fg, 75.60.Ch, 75.70.Kw, 87.15.hj

I. INTRODUCTION

The ability to manipulate the magnetization in a domain wall (DW) using a spin-polarized current has significant potential for novel spintronic devices and has attracted considerable attention from both experimental and theoretical researchers since its first introduction by Berger [1] and Slonczewski [2]. The spin-transfer torque resulting from the exchange interaction between the conduction electrons and the local magnetization is an important phenomenon with potential applications as spin-torque oscillators for telecommunications applications, in DW-based magnetic devices such as racetrack memory [3,4], and in the switching of magnetic random access memory (MRAM) elements [5,6]. It provides an exciting technological advance, coupling fast speed, nonvolatility, and low power requirements [7–9]. The physics of the spin-torque phenomenon can be described in terms of a spin accumulation, which interacts with the local magnetic moments via a quantum mechanical exchange interaction. The mechanism of spin-transfer torque in slowly varying magnetization, i.e., a domain wall, can be theoretically described by considering the spin current carried by the conduction electrons into the magnetic domain wall. The spin-transfer torque arising from the *s*-*d* exchange interaction acts on the spin current to adiabatically align it in the direction of the local magnetization. Simultaneously, a reaction torque proportional to the spin current density is created on the local magnetization within the DW. For sufficiently high spin current density, the spin injection causes the magnetization reorientation, resulting in the DW motion in the direction of conduction electron flow.

The spin-transfer torque can be decomposed into adiabatic and nonadiabatic contributions. The former, known as the Slonczewski torque, accounts for the conduction electrons' following the direction of local magnetization whereas the latter occurs with a rapid change in the magnetization, which has been explained by spin mistracking, momentum transfer, or spin-flip scattering [10]. In general, the nonadiabatic torque is assumed to be much weaker than the adiabatic torque [11,12]. The magnitudes of the adiabatic and nonadiabatic torques strongly depend on the DW width, which is determined by the anisotropy constant and exchange interaction of the material. The DW width becomes a significant factor for the spin-torque efficiency due to the fact that for a material with high anisotropy the resulting strong magnetization gradient within the DW subsequently gives rise to a high DW velocity. Therefore, the materials with a large anisotropy, which in turn allow a low current density to initiate DW motion, are promising candidates for the application in spintronic devices.

Spin torques are generally introduced into micromagnetic models via adiabatic and nonadiabatic terms proportional, respectively, to coefficients μ_x and β_x [11,13–15]. The magnitudes of both coefficients are generally taken as (unknown) constants (i.e., spatially independent) in the usual formalism and their magnitude is still a matter of discussion. Interestingly, a recent study by Claudio-Gonzalez *et al.* [11] has demonstrated that the magnitude of these coefficients strongly depends on the spatial variation of the magnetization gradient giving rise to the nonuniform behavior throughout the layer. This results in the divergence of the coefficients at positions with small gradient of magnetization. To avoid the consequent nonphysical behavior of the empirical constants μ_x and β_x Claudio-Gonzalez *et al.* [11] evaluated an effective nonadiabatic coefficient β_{diff} providing the description of nonadiabatic torque by averaging $|\partial M/\partial x|^2$ with a weight function. In our recent work [16], the spin-torque coefficients are calculated directly from the spin accumulation. The results show that the dynamic micromagnetic approach based on adiabatic and nonadiabatic terms with constant coefficients is valid only for systems with slow spatial variations of the magnetization.

In the present work, we calculate the spatial spin-transfer torque within the DW directly from the spin accumulation based on our recent work in Ref. [16] instead of calculating from the conventional model [11,13–15] through the spin-torque coefficients, which are unknown. Spin accumulation naturally includes the effect of both adiabatic and nonadiabatic

*phanwadeec@gmail.com

torques. This provides the new route of spin-torque calculation to get insight into the physical description behind the mechanism of current-induced domain wall motion and avoids various limitations of the conventional model in estimating the empirical constants, i.e., μ_x and β_x. Using this approach we have investigated the DW motion driven by the spin torque using the self-consistent solution of the spin accumulation and magnetization coupled with atomistic model. We find that the DW displacement and initial DW velocity strongly depend on the strength of the magnetocrystalline anisotropy and current density, and that the adiabaticity of the spin torque is dependent on the domain wall width.

II. METHODOLOGY

To investigate the domain wall motion driven by injecting spin-polarized current, the generalized spin accumulation model coupled with atomistic model is employed. Semianalytical solution of spin accumulation is applied to a series of layers representing the spatial variation of the magnetization in a domain wall to calculate the spin torque at any position of the system. Meanwhile, the atomistic model is used to investigate the dynamics of magnetization caused by spin torque. These two models are detailed in the following.

A. Spin accumulation model

The spin-transfer torque originating from the spin accumulation can be described via the *s-d* exchange interaction model [13,16,17]. The *s-d* model has been used to present a qualitative description of current-induced torque acting on spin moment. The exchange energy due to the interaction of the spin accumulation and the local spin moment is conventionally described by the Hamiltonian given by

$$\mathcal{H}_{\rm sd} = -J\mathbf{m}\cdot\mathbf{S}, \tag{1}$$

where $\mathbf{m}$ denotes the spin accumulation. $\mathbf{S}$ is the unit vector of the local spin moment and J is the exchange coupling strength between the spin accumulation and the local spin moment. To investigate the spin accumulation in the ferromagnet for any arbitrary direction of the spin moment, the general solution of the spin accumulation based on a transfer matrix approach as detailed in Ref. [16] will be employed.

In the rotated basis system $\hat{\mathbf{b}}_1$, $\hat{\mathbf{b}}_2$, and $\hat{\mathbf{b}}_3$, the component of spin accumulation is parallel and perpendicular to the local spin moment. The longitudinal component will be parallel to $\hat{\mathbf{b}}_1$ and the two components of the transverse spin accumulation along the directions $\hat{\mathbf{b}}_2$ and $\hat{\mathbf{b}}_3$. The general solution of spin accumulation can then be expressed in the following form

$$\begin{aligned}
\mathbf{m}_{\parallel}(x) &= m_{\parallel}(0)e^{-x/\lambda_{\rm sdl}}\hat{\mathbf{b}}_1\\
\mathbf{m}_{\perp,2}(x) &= 2e^{-k_1 x}[u\cos(k_2 x) - v\sin(k_2 x)]\hat{\mathbf{b}}_2\\
\mathbf{m}_{\perp,3}(x) &= 2e^{-k_1 x}[u\sin(k_2 x) + v\cos(k_2 x)]\hat{\mathbf{b}}_3,
\end{aligned} \tag{2}$$

with $(k_1 \pm ik_2) = \sqrt{\lambda_{\rm trans}^{-2} \pm i\lambda_J^{-2}}$, where $\lambda_J = \sqrt{2\hbar D_0/J}$. Here $\lambda_{\rm sdl}$ is the spin diffusion length, $\lambda_{\rm trans}$ is the transverse damping and D_0 the diffusion constant. $m_{\parallel}(0)$, u, and v are constants, which can be obtained by imposing continuity of the spin current at the interface. The spin accumulation in the rotated basis system can be expressed in the Cartesian coordinate system by using a transformation matrix [16].

The effect of the spin torque can be considered as an additional effective field arising from the *s-d* exchange interaction between the local spin moment and the spin accumulation, given by

$$\mathbf{H}_{\rm ST} = -\frac{\partial\mathcal{H}_{\rm sd}}{\partial\mathbf{S}} = J\mathbf{m}. \tag{3}$$

B. Atomistic spin model

We model the magnetization dynamics induced by the spin-transfer torque using an atomistic spin model coupled with the spin accumulation. The energetics of the system are described using a classical spin Hamiltonian with the Heisenberg form of the exchange interaction [18] written as

$$\mathcal{H} = -\sum_{i\neq j} J_{ij}\mathbf{S}_i\cdot\mathbf{S}_j - k_u\sum_i(\mathbf{S}_i\cdot\mathbf{e})^2 - |\mu_s|\sum_i \mathbf{S}_i\cdot\mathbf{H}_{\rm app}, \tag{4}$$

where J_{ij} is the nearest-neighbor exchange integral between spin sites i and j, $\mathbf{S}_i$ is the local normalized spin moment, $\mathbf{S}_j$ is the normalized spin moment of the neighboring atom at site j, k_u is the uniaxial anisotropy constant, $\mathbf{e}$ is the unit vector of the easy axis, and $|\mu_s|$ is the magnitude of the spin moment. The parameters of the model are representative of Co with a simplified simple cubic discretization, with an interatomic exchange energy $J_{ij} = 11.2\times10^{-21}$ J/link and $\mu_s = 1.44\mu_{\rm B}$ at 0 K.

The demagnetizing field is calculated at the micromagnetic level using the macrocell approach [18,19]. Each macrocell contains a predefined number of atomic unit cells and the net magnetization within the cell is determined by the average of the atomic spins in the cell. Macrocell moments (k,l) then interact using the dipole-dipole interaction including the self-demagnetizing term [18] given by

$$\mathbf{H}_{{\rm dip},k} = \frac{\mu_0}{4\pi}\sum_{l\neq k}\left[\frac{3(\boldsymbol{\mu}_l\cdot\hat{\mathbf{r}}_{kl})\hat{\mathbf{r}}_{kl} - \boldsymbol{\mu}_l}{|r_{kl}|^3}\right] - \frac{\mu_0}{3}\frac{\mu_k\hat{\mu}_k}{V}, \tag{5}$$

where $\boldsymbol{\mu}_l = \mu_s\sum_{i=1}^{n_{\rm atom}}\mathbf{S}_i$ is the vector of the magnetic moment in the macrocell site l, which is found from the summation of spin moments in the macrocell l, μ_0 is the permeability of free space, V is the volume of the macrocell, r_{kl} is the distance and $\hat{\mathbf{r}}_{kl}$ the corresponding unit vector between macrocell sites k and l, and $n_{\rm atom}$ is the number of atoms in each macrocell. The self-interaction term in Eq. (5) neglects the configurational anisotropy of the (cubic) macrocells. We approximate the dipole field as constant over the cell κ containing spin i. The effective local field acting on spin i is therefore given by

$$\mathbf{H}_{{\rm eff},i} = -\frac{1}{|\mu_s|}\frac{\partial\mathcal{H}}{\partial\mathbf{S}_i} + \mathbf{H}_{{\rm dip},\kappa}. \tag{6}$$

The dynamics of the spin system under the action of the spin-transfer torque can be modeled using the standard Landau-Lifshitz (LL) equation of motion with the inclusion of an additional spin-torque field ($J_{\rm sd}\mathbf{m}$) [13,20,21] as follows:

$$\frac{\partial\mathbf{S}}{\partial t} = -\gamma\mathbf{S}\times(\mathbf{H}_{\rm eff} + J_{\rm sd}\mathbf{m}) + \frac{\alpha}{\mu_s}\mathbf{S}\times\frac{\partial\mathbf{S}}{\partial t}. \tag{7}$$

For convenient numerical integration, we cast Eq. (7) into the Landau-Lifshitz-Gilbert (LLG) form, giving the final equation of motion

$$\frac{\partial \mathbf{S}}{\partial t} = -\frac{\gamma}{(1+\lambda^2)}\mathbf{S}\times(\mathbf{H}_{\rm eff}+J_{\rm sd}\mathbf{m}) - \frac{\gamma\lambda}{(1+\lambda^2)}\{\mathbf{S}\times[\mathbf{S}\times(\mathbf{H}_{\rm eff}+J_{\rm sd}\mathbf{m})]\}, \quad (8)$$

where γ is the absolute gyromagnetic ratio, $\lambda = 0.1$ is the intrinsic Gilbert damping constant applied at the atomic level, $\mathbf{S}$ is the normalized spin moment, and $\mathbf{H}_{\rm eff}$ is the effective field given by Eq. (6). The local effective field $\mathbf{H}_{\rm eff}$ leads to damped precessional motion into the direction of the local effective field. Interestingly, the additional field due to the presence of the injected spin current $J\mathbf{m}$ gives rise to the contribution of adiabatic and nonadiabatic torques. This term describes the spin-torque effect on the spin motion and indicates that the additional field due to the spin-transfer torque can be another source of precession and damping [22,23]. We note that all simulations are done without thermal fluctuations, that is, at zero K using the VAMPIRE software package [18].

C. Spin-torque calculation

To calculate the adiabatic (AST) and nonadiabatic spin torques (NAST), let us consider the rotated basis system where the local spin moment in the current layer ($\mathbf{S}$) is along the $\hat{\mathbf{b}}_1$ direction whereas that in the previous layer is oriented in the plane $\hat{\mathbf{b}}_1\hat{\mathbf{b}}_2$. The spin moment in the previous layer can be rotated into the basis coordinate system as illustrated in Fig. 1, $\mathbf{S}_p = S_{p\parallel}\hat{\mathbf{b}}_1 + S_{p\perp}\hat{\mathbf{b}}_2$, by using the transformation matrix given by

$$[S_{\rm basis}] = [T]^{-1}[S_{\rm global}], \quad (9)$$

and the transformation matrix is as follows

$$[T] = \begin{bmatrix} \frac{S_xX''+S_yY''}{D_2D_3} & \frac{X''}{D_2^2D_3} - \frac{S_xS_yY''}{D_1D_2D_3} & \frac{S_zY''}{D_1D_3} \\ \frac{-S_xY''+S_yX''}{D_2D_3} & \frac{Y''}{D_2^2D_3} - \frac{S_xS_yX''}{D_1D_2D_3} & \frac{S_zX''}{D_1D_3} \\ \frac{S_z}{D_1} & \frac{-S_xS_z}{D_1D_2} & \frac{-S_y}{D_1} \end{bmatrix} \quad (10)$$

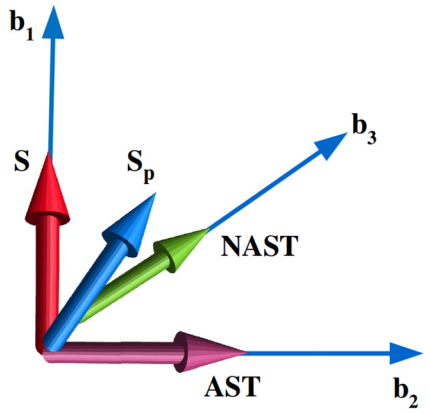

FIG. 1. (Color online) Schematic representation of the spin-transfer torque consisting of the adiabatic (AST) and nonadiabatic (NAST) torques in the rotated basis system.

with

$$\begin{bmatrix} X'' \\ Y'' \\ Z'' \end{bmatrix} = \begin{bmatrix} \frac{S_{p,x}D_1^2 - S_x(S_yS_{p,y}+S_zS_{p,z})}{D_1D_2} \\ \frac{S_zS_{p,y}-S_yS_{p,z}}{D_1} \\ \frac{S_xS_{p,x}+S_yS_{p,y}+S_zS_{p,z}}{D_2} \end{bmatrix}, \quad (11)$$

where $[S_{\rm basis}]$ and $[S_{\rm global}]$ are the spin moments in the basis coordinate system and in the global coordinate system respectively. S_x, S_y, and S_z are the x, y, and z components of spin moment in the current layer, respectively. $D_1 = \sqrt{S_y^2+S_z^2}$, $D_2 = \sqrt{S_x^2+S_y^2+S_z^2}$, and $D_3 = \sqrt{X''^2+Y''^2}$.

In the basis system as shown in Fig. 1, the adiabatic and nonadiabatic torques can be determined from the total spin torque $\tau_{\rm ST}$ via the s-d exchange interaction as follows

$$\begin{aligned} \tau_{\rm ST} &= S\times J_{\rm sd}\mathbf{m} \\ &= \hat{\mathbf{b}}_1\times J_{\rm sd}(m_\parallel\hat{\mathbf{b}}_1 + m_{\perp,2}\hat{\mathbf{b}}_2 + m_{\perp,3}\hat{\mathbf{b}}_3) \\ &= -J_{\rm sd}m_{\perp,3}\hat{\mathbf{b}}_2 + J_{\rm sd}m_{\perp,2}\hat{\mathbf{b}}_3. \end{aligned} \quad (12)$$

In general, the AST is the in-plane torque whereas the NAST is introduced as the fieldlike torque or the out-of-plane torque. Therefore, the spin moments in the rotated basis system as illustrated in Fig. 1 results in the AST and NAST along the directions of $\hat{\mathbf{b}}_2$ and $\hat{\mathbf{b}}_3$, respectively. As a consequence, the AST and NAST in the rotated basis system are given by

$$\begin{aligned} \tau_{\rm AST} &= -J_{\rm sd}m_{\perp,3}\hat{\mathbf{b}}_2 \\ \tau_{\rm NAST} &= J_{\rm sd}m_{\perp,2}\hat{\mathbf{b}}_3. \end{aligned} \quad (13)$$

The above equation shows that the AST and NAST can be accessed directly via the spin accumulation. Subsequently, the dynamics of spin motion including the effect of the spin-transfer torque can be investigated by employing Eq. (8).

III. CURRENT-INDUCED DOMAIN WALL MOTION

In this work we investigate the dynamics of the magnetization in a bilayer system consisting of two ferromagnets (FMs). The current-induced domain wall motion is studied by injecting a spin current perpendicular to the plane of the bilayer. In this computational study, the investigation is presented in two sections. First, the effect of the spin-transfer torque on the DW dynamics is studied, followed by an investigation of the time evolution of DW displacement and DW velocity. Furthermore, the effect of the current density (j_e) is also studied by injecting currents with different magnitudes. This allows the investigation of the critical current density which is the minimum spin current required to move the domain wall. Second, the effect of the DW width on the time evolution of the DW displacement and DW velocity is considered.

A. Time evolution of magnetization and spin torque

The system consists of a bilayer structure with a pinned layer (PL) providing a spin-polarized current (which is not modeled explicitly) and a free layer (FL) with dimensions of 60 nm×30 nm×1.5 nm. In order to calculate the spin accumulation and spin torque the system is discretized into macrocells 1.5 nm×1.5 nm×1.5 nm in size.

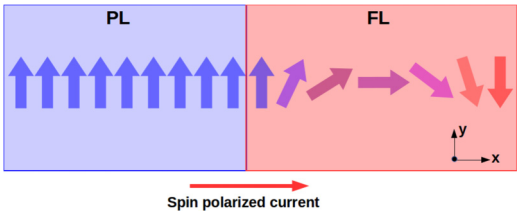

FIG. 2. (Color online) The the tail-to-tail domain wall contained in the second ferromagnet of the bilayer system with the uniaxial anisotropy constant of $k_u = 2.52\times10^6$ J/m^3: The arrows indicate the direction of magnetization. The magnetization along the y direction is represented by the blue coloring. In contrast, the red color shows the orientation of magnetization in the $-y$ direction.

The magnetic moment in each macrocell is then calculated by averaging over the spins within the cell. The pinned layer is not considered explicitly; its role is simply to provide a spin-polarized current through the layer under investigation. A domain wall is forced into the free layer by fixing an antiparallel magnetization configuration at the boundaries of the system as illustrated in Fig. 2. The DW profile is transverse in the xy plane. The studied system is based on a material with a uniaxial anisotropy constant of $k_u = 2.52\times10^6$ J/m^3 $\equiv$ 2.7×10^{-23} J/atom with the y direction as the easy axis and a lattice constant of $a = 3.49$ Å. The transport parameters of Co used in spin accumulation calculation are taken from Ref. [21] as the following values, $\beta = 0.5, \beta' = 0.9$, $D_0 = 0.001$ m^2/s, $\lambda_{\rm sdl} = 60$ nm, and $\lambda_J = 3$ nm.

We first investigate the effect of the spin-transfer torque on the domain wall motion by introducing a current density of 50 MA/cm^2 into the bilayer system. The current-induced domain wall motion can be observed through the components of magnetization. Figure 3 shows the time evolution of the magnetization after the application of the current induced by the spin-torque. In the absence of the spin-transfer torque at $t = 0$ ns, the DW is situated centrally and the position of the DW center is defined by the maximum magnetization of the x component and zero of the y component. In interpreting the numerical results it is necessary to stress that the DW can initially move freely but, due to the finite system size, after some time interacts with the strong pinning sites at the boundaries, which are used to inject the DW into the system. The DW initially moves when the spin current is injected above the critical value. The DW has a translational motion to the right, which is the direction of the injected current and it tends to stop moving at the equilibration time $t = 0.6$ ns with a finite DW displacement, as expected given its interaction with the boundary pinning sites. Specifically, a small out-of-plane or z component develops during the propagation time. Its appearance comes from the fact that the domain wall interacts with the strong pinning site. This is evidence of DW deformation due to interaction with the pinning site. The DW deformation and the occurrence of z component exhibited in this study are in good agreement with the recent experimental and theoretical studies [24–26].

We next consider the time variation of the spin-transfer torque via self-consistent solution of the magnetization and spin accumulation, naturally including the adiabatic and nonadiabatic torques, to understand its dependence on the

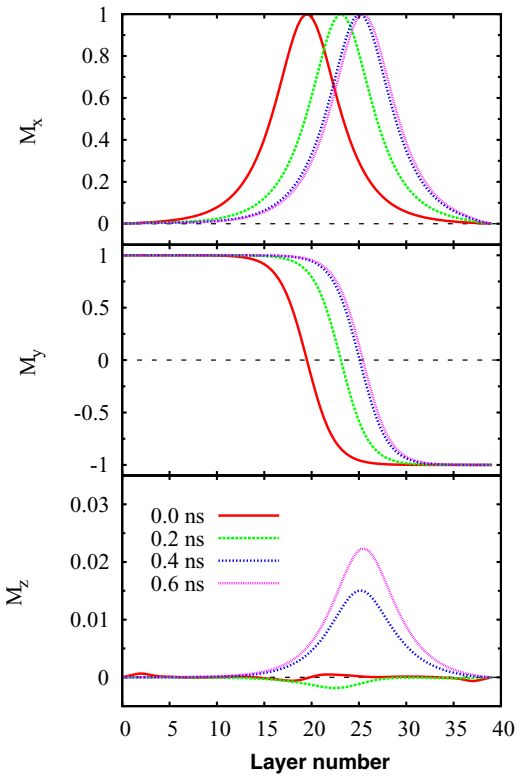

FIG. 3. (Color online) Schematic representation of the magnetization component with time evolution from 0 ns to the equilibration time of 0.6 ns: The current density injected into the bilayer system containing the DW is 50 MA/cm^2.

magnetic structure and its time evolution. The x and y components give the adiabatic torque, which tends to develop towards the direction of magnetization. On the other hand the z component arises from the contribution of the nonadiabatic torque, which acts out of the plane. The spin torque acting on the local magnetization due to the spin-polarized current results in the translation of the DW. As a consequence, the spatial spin torque at different times as illustrated in Fig. 4 reflects the spatial magnetization configuration of Fig. 3, which is translated due to the spin torque. It is found that the motion ceases after 0.6 ns as the DW contacts with the boundary pinning sites. In addition, in this case the magnitude of the adiabatic and nonadiabatic torques remain constant with time and the domain wall width is not significantly affected as the wall contacts the boundary pinning sites, suggesting that the spin current density of 50 MA/cm^2 is not high enough to distort the pinned DW.

B. DW displacement and velocity

We next consider the effect of the current density on the domain wall motion. This leads to the investigation of the critical spin current density (j_e), required to initiate domain wall motion and also spin-torque driven oscillations of the magnetization of the DW fixed at the strong boundary pinning sites. It is first noted that the calculation in this section observed the domain wall motion in the bilayer system with the anisotropy constant of $k_u = 2.52\times10^6$ J/m^3 giving rise to the

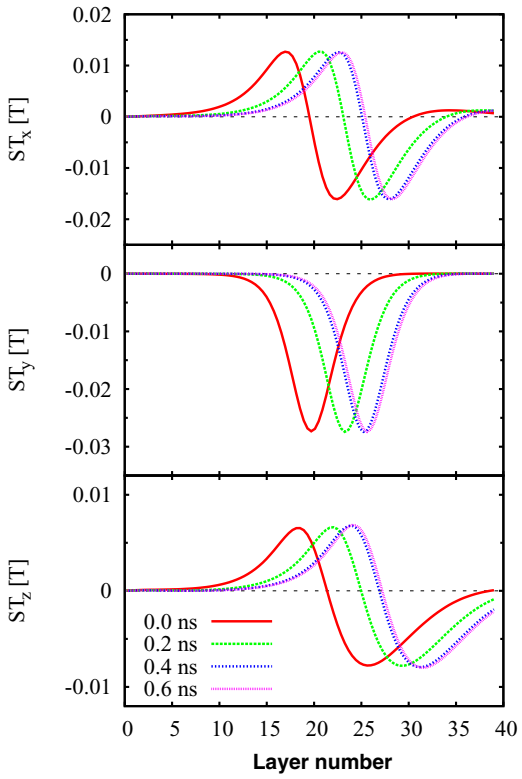

FIG. 4. (Color online) The time evolution of the spatial spin-transfer torque with $j_e = 50\,\mathrm{MA/cm}^2$.

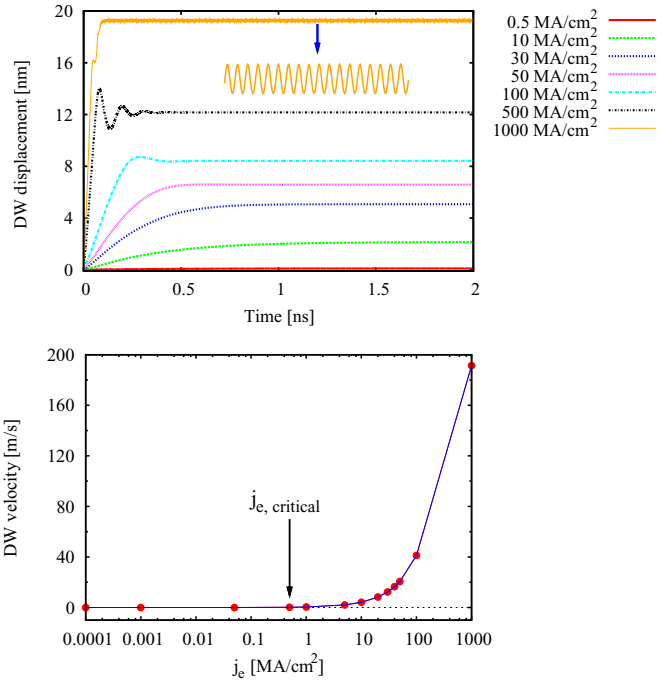

FIG. 5. (Color online) (Top) The time variation of domain wall displacement with different current densities. (Bottom) The initial DW velocity as a function of current density: The critical current density, minimum current density required to move DW is 0.5 $\mathrm{MA/cm}^2$.

domain wall width of approximately 6.86 nm. The application of the spin-polarized current induces a displacement of the DW position with time, as shown in Fig. 5 (top panel). The DW displacement is monitored by observing the shift of the DW center from the initial position at each time step. It can be seen that the DW displacement is time dependent and increases linearly in the first time period before reaching a steady state with finite displacement due to the interaction with the boundary pinning sites [24,27,28]. The equilibration time of DW displacement tends to decrease with increasing spin current density, consistent with the increased DW velocity.

To describe the behavior of the DW displacement with different regimes of the current density, it is important to consider the critical current density, which can be evaluated through the initial DW velocity. The initial velocity is calculated by determining the rate of change of the DW displacement in the first 0.1 ns as the DW shows uniform translational motion during that period. The relation between the initial DW velocity as a function of the current density is plotted on a semilogarithmic scale in Fig. 5 (bottom panel). It is found that the critical current density is 0.5 $\mathrm{MA/cm}^2$. This behavior is also found in the previous studies [26,29–33].

On increasing the current density above the critical value, the domain wall moves uniformly without any precession along the direction of the injected spin current. This motion induced by the spin current is due to the conservation of the angular momentum. At high spin current density, the domain wall motion is accompanied by oscillatory behavior, which tends to be observed with a high current density over $100\,\mathrm{MA/cm}^2$. Interestingly, at extremely high values of current density $j_e = 1000\,\mathrm{MA/cm}^2$, the DW reaches the boundary inning sites and the translational motion stops. At this point the dynamic behavior of the DW is becomes oscillatory, exhibiting a stable precessional state around a finite wall displacement [27]. At equilibrium, the DW displacement oscillates at a high frequency of 300 GHz since the pinned DW essentially acts as a spin-torque oscillator. This also implies the appearance of an out-of-plane component of magnetization resulting from the nonadiabatic torque, consistent with the previous studies [34,35]. Our result with the current density of $j_e = 1000\,\mathrm{MA/cm}^2$ yielding the initial velocity at approximately 200 m/s is in good agreement with the analytical results of the one-dimensional (1D) Walker ansatz model in Ref. [36] where the domain displacement at equilibrium is about 18 nm. However, the oscillatory behavior cannot be observed in 1D model because the effect of nonadiabatic spin torque is not taken into account.

In order to understand the origin of the oscillatory behavior, the magnetization component at the initial DW center is investigated in its time evolution after the introduction of the spin-transfer torque. Figure 6 clearly shows that the spin-transfer torque causes the deformation of the DW leading to precessional motion of the x and z components. This is the precession of the equilibrium magnetization about the effective field determined by the interaction with the pinning site. The nonadiabatic torque driving the DW in the stable precessional state is strong enough to deform the Néel wall so as to have a significant out-of-plane component, which results in the oscillatory behavior. The domain wall motion accompanied by the precessions due to the nonadiabatic torque has been confirmed by recent studies [10,25,27,35,37]. Interestingly,

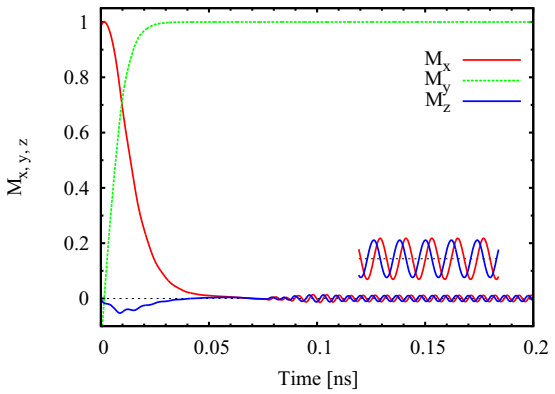

FIG. 6. (Color online) The magnetization component of the initial DW center with time evolution after injecting the spin current with the density of 1000 MA/cm^2.

the observed oscillatory motion of the domain wall for large current is similar to the behavior of domain walls at currents above the Walker threshold.

IV. CURRENT-INDUCED DW MOTION: EFFECT OF THE DOMAIN WALL WIDTH

We now turn to the effect of the domain wall width on the magnetization dynamics. This is investigated by introducing a spin-polarized current into a bilayer system containing a domain wall whose width is varied by changing the anisotropy constant. The domain wall profile with different anisotropy constants can be seen in Fig. 7. The magnetization is allowed to vary continuously throughout, constrained by pinning sites at the boundaries. The width of the domain wall is varied by increasing the uniaxial anisotropy constant to investigate the influence of the magnetic anisotropy on the spin-transfer torque on the domain wall. The anisotropy constant is varied from the typical anisotropy value of cobalt $k_u = 4.2\times10^5$ J/m^3 up to 10 times that value. The x and y components of magnetization can be used to characterize the center of DW and the DW width. The z component of the magnetization is zero according to the usual properties of the Néel wall for the thin sample. A detailed qualitative investigation of the current-induced DW motion with the effect of anisotropy constant will be discussed in the following.

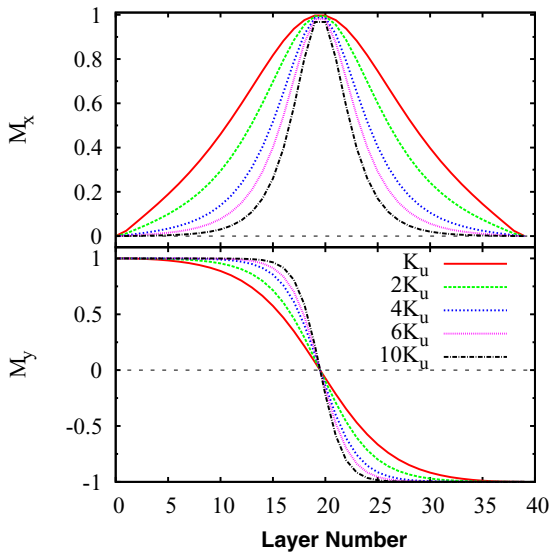

FIG. 7. (Color online) The domain wall profile transverse in the xy plane with various anisotropy constants: The uniaxial anisotropy constant of cobalt is $K_u = 4.2\times10^5$ J/m^3. The distance between layer is given in units of supercells, corresponding to five atomic spacings.

A. DW displacement and velocity

First, a spin current with the density of 50 MA/cm^2 is injected into the bilayer system along the x direction in order to observe the manipulation of the magnetization within the DW with different anisotropy constants. The magnetization configuration after the introduction of the spin current for 1 ns is illustrated in Fig. 8. It shows that the DW motion is initiated after injecting the spin current into the system. The center of the domain wall moves from the initial position along the direction of the spin current. The system with high anisotropy is easily displaced due to a larger gradient of magnetization within the DW giving rise to a high magnitude of spin torque acting on it. Interestingly, the DW center position of the system with the anisotropy constant of k_u is unchanged. This implies that the density of spin current injected to the system is below

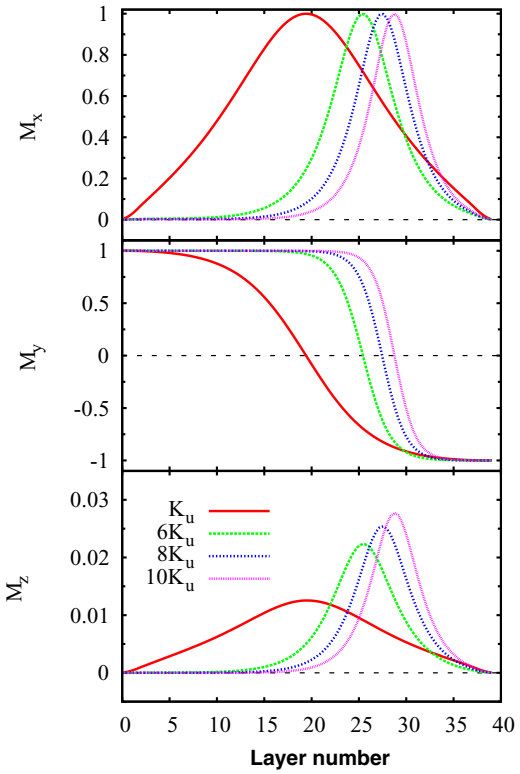

FIG. 8. (Color online) The component of magnetization in the second FM with various anisotropy constants after the introduction of the spin current for 1 ns: The center of the DWs are displaced in the direction of injected spin current. The system with high anisotropy constant leading to a large gradient of magnetization within domain wall results in a large displacement of the DW.

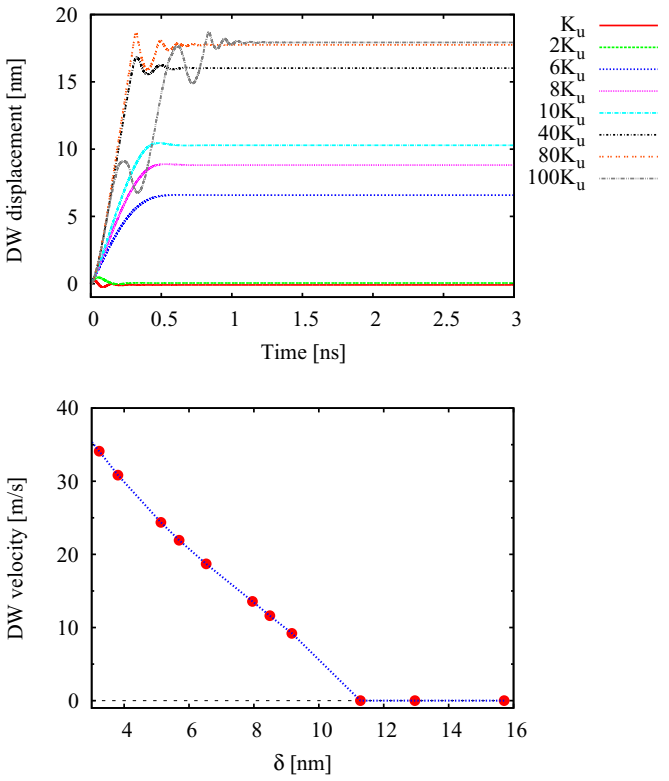

FIG. 9. (Color online) (top) The time-dependent variation of the domain wall displacement and (bottom) the initial domain wall velocity of different uniaxial anisotropy systems with the spin current density of 50 MA/cm^2.

the critical value, which depends on the DW width [38–40]. In addition, the out-of-plane component is likely to be large for high anisotropy.

Furthermore, it is also worthwhile to observe the dynamic behavior of the DW motion via the DW displacement and the initial DW velocity. As illustrated in Fig. 9 (top panel), the DW displacement is not noticeable for a very wide wall, specifically for uniaxial anisotropy constants of k_u and $2k_u$. The DW exhibits transient oscillatory behavior back to it initial position. Hence, higher spin current density is needed in order to initiate the translation of DW for these cases. On the other hand, displacement of the narrow DW tends to be more easily initiated than the wide DW. This is because of the strong interaction between the spin current and the local magnetization gradient within the DW giving rise to a large spin-transfer torque. For a low anisotropy, the linear response of the DW displacement occurs in the first 0.1 ns and then reaches the equilibrium state after reaching the boundary pinning sites. For a high anisotropy, the DW displacement deviates from linear behavior and the precessional motion is enhanced for several cycles in the first ns before reaching the equilibrium state. The deviation from the linear behavior in the first period becomes stronger for higher anisotropy. In the case of this spin current density, the stable precessional state is not established as the current density is not high enough to push the DW against the boundary pinning sites.

Finally, we consider the initial DW velocity as a function of the DW width. Clearly the initial DW velocity depends sensitively on the DW width as can be seen in Fig. 9 (bottom panel). The initial DW velocity decreases with increasing DW width as a result of the decreasing magnetization gradient. The similar result has been shown in Ref. [41]. This relation can be used to evaluate the critical DW width for each spin current density. The current density of 50 MA/cm^2 is able to move a DW along the direction of the injected spin current in case of the DW width less than 11.2 nm.

B. Spin-transfer torque

We now consider the spin-transfer torque consisting of adiabatic (AST) and nonadiabatic (NAST) components. As mentioned before, the total spin-transfer torque is mainly contributed by the AST resulting from the spin accumulation component following the direction of the local magnetization whereas the out-of-plane torque comes from the NAST arising from the electron mistracking. The strength of the spin-transfer torque on the DW can be represented by considering the maximum value occurring at any position over the DW region given that its contribution is nonuniform throughout the DW. In addition, the degree of nonadiabatic torque or the so-called nonadiabaticity (D_{NAST}), which characterizes the relative influence of the NAST on the DW compared with the AST, is also evaluated by the following equation,

$$D_{\mathrm{NAST}} = \frac{|\mathrm{NAST}_{\mathrm{max}}|}{|\mathrm{AST}_{\mathrm{max}}|}. \tag{14}$$

$|\mathrm{NAST}_{\mathrm{max}}|$ and $|\mathrm{AST}_{\mathrm{max}}|$ are the maximum value of adiabatic and nonadiabatic torques within DW.

Clearly, as shown in Fig. 10, both adiabatic and nonadiabatic torques tend to be more effective in narrow domain walls due to the large gradient of the magnetization. It can also be seen that the nonadiabaticity factor becomes more significant for a small DW width. This is schematically shown in Fig. 10. In contrast, the pure adiabatic torque is likely to dominate the total torque, with negligible nonadiabatic torque, for a large DW width. This is consistent with previous studies [14,41,42]. The results also indicate that the nonadiabatic torque, which is represented by the value of β used in the micromagnetic approach is directly dependent on the DW width. In the case

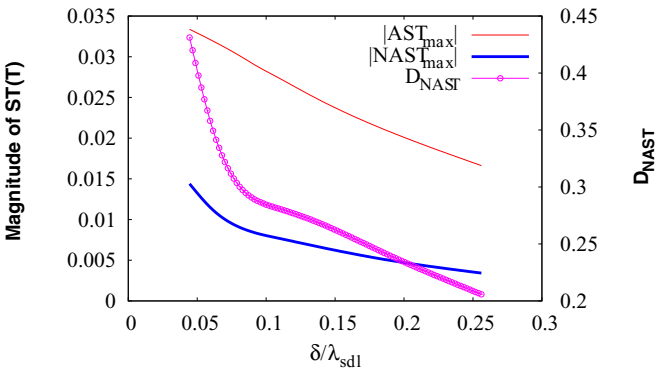

FIG. 10. (Color online) The thickness dependence of a maximum of adiabatic spin torque (AST), nonadiabatic spin torque (NAST) and the degree of nonadiabaticity (D_{NAST}): The spin diffusion length (λ_{sdl}) is 60 nm.

of $\delta \ll \lambda_{\mathrm{sdl}}$, the nonadiabatic torque becomes significant to the system.

V. CONCLUSION

In this work we have applied the modified formalism of spin accumulation with an atomistic spin model to study the dynamics of a DW in the presence of a spin-transfer torque. The model uses a transfer matrix approach to determine directly the equilibrium spin accumulation avoiding the need for computationally expensive time stepping of the equation of motion. Domain wall dynamics under the influence of a spin-polarized current are studied by self-consistent calculations of the spin accumulation and magnetization. The spin accumulation is calculated in a rotated basis, which gives access to both the adiabatic and nonadiabatic contributions to the spin torque, which arise naturally in the model. The total spin torque contributed by adiabatic and nonadiabatic torques at any position within the DW is considered. The results indicate that both torques are inversely proportional to domain wall width. Furthermore, it is found that the adiabatic torque dominates the total spin torque; meanwhile the nonadiabatic torque controls the out-of-plane component of spin torque. The dependence of spin torque on the DW width is consistent with the proportionality of the spin torque to the gradient of the magnetization. However, it is important to note that the self-consistent solution of spin accumulation and magnetization leads to a further contribution to the effect of the DW width. Specifically, we show that the adiabatic and nonadiabatic components of the spin torque reduce with increasing DW width relative to the spin diffusion length, which becomes an important characteristic length in the calculation of the spin torque. Both components decrease at different rates, with the result that the nonadiabaticity factor, indicative of the relative strength of the nonadiabatic torque, tends to decay to zero as the DW width increases. Our results show that materials with high anisotropy such as FePt giving rise to narrow domain wall are more effective for data storage application involving DW propagation, such as racetrack memories [43], due to the enhancement of high spin-transfer torque. We also conclude that the spin torque is strongly dependent on the spin diffusion length, which is an important factor in materials design.

ACKNOWLEDGMENT

P.C. would like to acknowledge financial support from Mahasarakham University, Thailand.

[1] L. Berger, Emission of spin waves by a magnetic multilayer traversed by a current, Phys. Rev. B **54**, 9353 (1996).

[2] J. C. Slonczewski, Current-driven excitation of magnetic multilayers, J. Magn. Magn. Mater. **159**, L1 (1996).

[3] S. S. P. Parkin, M. Hayashi, and L. Thomas, Magnetic Domain-Wall Racetrack Memory, Science **320**, 190 (2008).

[4] L. Thomas, R. Moriya, C. Rettner, and S. S. Parkin, Dynamics of Magnetic Domain Walls Under Their Own Inertia, Science **330**, 1810 (2010).

[5] S. Tehrani, E. Chen, M. Durlam, M. DeHerrera, J. Slaughter, J. Shi, and G. Kerszykowski, High density submicron magnetoresistive random access memory (invited), J. Appl. Phys. **85**, 5822 (1999).

[6] H. Boeve, C. Bruynseraede, J. Das, K. Dessein, G. Borghs, J. De Boeck, R. Sousa, L. Melo, and P. Freitas, Technology assessment for the implementation of magnetoresistive elements with semiconductor components in magnetic random access memory (mram) architectures, IEEE Trans. Magn. **35**, 2820 (1999).

[7] M. Hosomi, H. Yamagishi, T. Yamamoto, K. Bessho, Y. Higo, K. Yamane, H. Yamada, M. Shoji, H. Hachino, C. Fukumoto, H. Nagao, and H. Kano, A novel nonvolatile memory with spin torque transfer magnetization switching: Spin-ram, in *Proceedings of the IEEE International Electron Devices Meeting, 2005, IEDM Technical Digest, Washington, DC* (IEEE, New York, 2005), pp. 459–462.

[8] S. Ikeda, K. Miura, H. Yamamoto, K. Mizunuma, H. D. Gan, M. Endo, S. Kanai, J. Hayakawa, F. Matsukura, and H. Ohno, A perpendicular-anisotropy cofebmgo magnetic tunnel junction, Nat. Mater. **9**, 721 (2010).

[9] D. Houssameddine, U. Ebels, B. Delaet, B. Rodmacq, I. Firastrau, F. Ponthenier, M. Brunet, C. Thirion, J.-P. Michel, L. Prejbeanu-Buda, M.-C. Cyrille, O. Redon, and B. Dieny, Spin-torque oscillator using a perpendicular polarizer and a planar free layer, Nat. Mater. **6**, 447 (2007).

[10] C. Burrowes, A. P. Mihai, D. Ravelosona, J.-V. Kim, C. Chappert, L. Vila, A. Marty, Y. Samson, F. Garcia-Sanchez, L. D. Buda-Prejbeanu, I. Tudosa, E. E. Fullerton, and J.-P. Attane, Non-adiabatic spin-torques in narrow magnetic domain walls, Nat. Phys. **6**, 17 (2010).

[11] D. Claudio-Gonzalez, A. Thiaville, and J. Miltat, Domain Wall Dynamics under Nonlocal Spin-Transfer Torque, Phys. Rev. Lett. **108**, 227208 (2012).

[12] R. Wieser, E. Y. Vedmedenko, and R. Wiesendanger, Indirect Control of Antiferromagnetic Domain Walls with Spin Current, Phys. Rev. Lett. **106**, 067204 (2011).

[13] S. Zhang, P. M. Levy, and A. Fert, Mechanisms of Spin-Polarized Current-Driven Magnetization Switching, Phys. Rev. Lett. **88**, 236601 (2002).

[14] J. Xiao, A. Zangwill, and M. D. Stiles, Spin-transfer torque for continuously variable magnetization, Phys. Rev. B **73**, 054428 (2006).

[15] P. Baláž, V. K. Dugaev, and J. Barnaś, Spin-transfer torque in a thick néel domain wall, Phys. Rev. B **85**, 024416 (2012).

[16] P. Chureemart, I. D'Amico, and R. W. Chantrell, Model of spin accumulation and spin torque in spatially varying magnetization structures: Limitations of the micromagnetic approach, J. Phys.: Condens. Matter **27**, 146004 (2015).

[17] S. Zhang and Z. Li, Roles of Nonequilibrium Conduction Electrons on the Magnetization Dynamics of Ferromagnets, Phys. Rev. Lett. **93**, 127204 (2004).
[18] R. F. L. Evans, W. J. Fan, P. Chureemart, T. A. Ostler, M. O. A. Ellis, and R. W. Chantrell, Atomistic spin model simulations of magnetic nanomaterials, J. Phys.: Condens. Matter **26**, 103202 (2014).
[19] E. Boerner, O. Chubykalo-Fesenko, O. Mryasov, R. Chantrell, and O. Heinonen, Moving toward an atomistic reader model, IEEE Trans. Magn. **41**, 936 (2005).
[20] P. M. Levy, The role of spin accumulation in current-induced swithcing of magnetic layers, or the first 10^{-12} s in a magnetic multilayer after the current is switched on, J. Phys. D: Appl. Phys. **35**, 2448 (2002).
[21] A. Shpiro, P. M. Levy, and S. Zhang, Self-consistent treatment of nonequilibrium spin torques in magnetic multilayers, Phys. Rev. B **67**, 104430 (2003).
[22] Z. Li and S. Zhang, Magnetization dynamics with a spin-transfer torque, Phys. Rev. B **68**, 024404 (2003).
[23] S. Takahashi and S. Maekawa, Spin current, spin accumulation and spin hall effect, Sci. Technol. Adv. Mater. **9**, 014105 (2008).
[24] P. D. Sacramento, L. C. Fernandes Silva, G. S. Nunes, M. A. N. Araújo, and V. R. Vieira, Supercurrent-induced domain wall motion, Phys. Rev. B **83**, 054403 (2011).
[25] D. M. Burn and D. Atkinson, Suppression of walker breakdown in magnetic domain wall propagation through structural control of spin wave emission, Appl. Phys. Lett. **102**, 242414 (2013).
[26] S.-H. Yang, K.-S. Ryu, and S. Parkin, Domain-wall velocities of up to 750ms1 driven by exchange-coupling torque in synthetic antiferromagnets, Nat. Nano **10**, 221 (2015).
[27] D. Hinzke and U. Nowak, Domain Wall Motion by the Magnonic Spin Seebeck Effect, Phys. Rev. Lett. **107**, 027205 (2011).
[28] X.-g. Wang, G.-h. Guo, Y.-z. Nie, G.-f. Zhang, and Z.-x. Li, Domain wall motion induced by the magnonic spin current, Phys. Rev. B **86**, 054445 (2012).
[29] J. Curiale, A. Lematre, T. Niazi, G. Faini, and V. Jeudy, Joule heating and current-induced domain wall motion, J. Appl. Phys. **112**, 103922 (2012).
[30] N. Vernier, J. P. Adam, A. Thiaville, V. Jeudy, A. Lemaître, J. Ferré, and G. Faini, Modified current-induced domain-wall motion in gamnas nanowires, Phys. Rev. B **88**, 224415 (2013).
[31] F.-S. Wu, L. Horng, Y.-M. Kao, H.-H. Chen, and J.-C. Wu, Modeling on current-induced multiple domain-wall motion in permalloy nanowires, Jpn. J. Appl. Phys. **53**, 093002 (2014).
[32] E. Martinez, S. Emori, N. Perez, L. Torres, and G. S. D. Beach, Current-driven dynamics of dzyaloshinskii domain walls in the presence of in-plane fields: Full micromagnetic and one-dimensional analysis, J. Appl. Phys. **115**, 213909 (2014).
[33] O. Boulle, L. D. Buda-Prejbeanu, E. Ju, I. M. Miron, and G. Gaudin, Current induced domain wall dynamics in the presence of spin orbit torques, J. Appl. Phys. **115**, 17 (2014).
[34] Z. Li and S. Zhang, Domain-Wall Dynamics and Spin-Wave Excitations with Spin-Transfer Torques, Phys. Rev. Lett. **92**, 207203 (2004).
[35] R. Sbiaa and R. W. Chantrell, Domain wall oscillations induced by spin torque in magnetic nanowires, J. Appl. Phys. **117**, 053907 (2015).
[36] Z. Li and S. Zhang, Domain-wall dynamics driven by adiabatic spin-transfer torques, Phys. Rev. B **70**, 024417 (2004).
[37] D. M. Burn, M. Chadha, S. K. Walton, and W. R. Branford, Dynamic interaction between domain walls and nanowire vertices, Phys. Rev. B **90**, 144414 (2014).
[38] S. Emori and G. S. D. Beach, Enhanced current-induced domain wall motion by tuning perpendicular magnetic anisotropy, Appl. Phys. Lett. **98**, 132508 (2011).
[39] D.-H. Kim, S.-C. Yoo, D.-Y. Kim, K.-W. Moon, S.-G. Je, C.-G. Cho, B.-C. Min, and S.-B. Choe, Maximizing domain-wall speed via magnetic anisotropy adjustment in pt/co/pt films, Appl. Phys. Lett. **104**, 142410 (2014).
[40] P. E. Roy and J. Wunderlich, In-plane magnetic anisotropy dependence of critical current density, walker field and domain-wall velocity in a stripe with perpendicular anisotropy, Appl. Phys. Lett. **99**, 122504 (2011).
[41] C. A. Akosa, W.-S. Kim, A. Bisig, M. Kläui, K.-J. Lee, and A. Manchon, Role of spin diffusion in current-induced domain wall motion for disordered ferromagnets, Phys. Rev. B **91**, 094411 (2015).
[42] M. Eltschka, M. Wötzel, J. Rhensius, S. Krzyk, U. Nowak, M. Kläui, T. Kasama, R. E. Dunin-Borkowski, L. J. Heyderman, H. J. van Driel, and R. A. Duine, Nonadiabatic Spin Torque Investigated using Thermally Activated Magnetic Domain Wall Dynamics, Phys. Rev. Lett. **105**, 056601 (2010).
[43] S. Parkin, Shiftable magnetic shift register and method of using the same, U.S. Patent No. 6,834,005 (December, 2004).